https://doi.org/10.53964/jmge.2023005

https://www.innovationforever.com

Journal of Modern Green Energy

ISSN 2790-3206 (Online)

Open Access

Research Article

An Assessment of Solar Driven Combined Cooling, Heating, and Electric Power Generation System: Using Energy, Exergy, and CO_2 Mitigation Approach

Mohd Parvez[1*], Shiv Lal[2], Osama Khan[3], Haidar Howari[4], Suhail Ahmad Siddiqui[1]

[1]Department of Mechanical Engineering, Al-Falah University, Faridabad, Haryana, India

[2]Department of Mechanical Engineering, Rajasthan Technical University, Kota, India

[3]Department of Mechanical Engineering, Jamia Millia Islamia, New Delhi, India

[4]Department of Physics, Deanship of Educational Services, Qassim University, Buraidah, Saudi Arabia

[*]**Correspondence to: Mohd Parvez, PhD, Professor,** Department of Mechanical Engineering, Al-Falah University, Faridabad, Haryana 121004, India; Email: mparvezalig@rediffmail.com

Received: February 23, 2023 **Revised:** April 3, 2023 **Accepted:** April 27, 2023 **Published:** May 25, 2023

Abstract

Background: Concentrated solar power (CSP) technology has been gaining more and more attention due to its inherent sustainable merit. Further promotion of sustainability requires the effective utilization of concentrated solar thermal radiations which can achieve through combined cooling, heat and power. In this context, the key objective of the research carried out in the present study was to propose and develop a novel solar thermal-driven combined cooling, heating, and power system for producing power of 7MW.

Objective: The objective of the study is to reduce heat loss at various places and to increase the overall energy and exergy of efficienices the system. The effect of very influencing parameters like direct normal irradiance (DNI), extraction pressure, turbine back pressure, turbine inlet pressure, and pump inlet temperature were ascertained on energy and exergy efficiencies for the trigeneration system. In addition, the model was extended to incorporate the evaluation to identify the causes and locations of thermodynamic imperfections. The energy and exergy efficiency and destruction were also evaluated.

Methods: For this study, a solar-driven combined cooling, heating, and electric power generation system is called the trigeneration system was designed by coupling a solar-based heliostat and centralized solar receiver with a conventional Rankine-based cycle. The conventional Rankine cycle comprises a basic heat recovery generator, a steam turbine, a condenser, and eventually a pump.

A thermodynamic model was developed which presented the analysis of various thermodynamic-based parameters of the integrated system comprising a solar-driven absorption refrigeration cycle. The analysis is formulated based on a cascaded system that grabs the energy and exergy-based methods in which the mass, energy, and exergy are balanced.

https://doi.org/10.53964/jmge.2023005

Results: The system was run for the solar radiation range from 600 to 1000W/m^2. It is found that the overall efficiency of the trigeneration system increases by 32 to 35% when DNI changed from 600 to 1000W/m^2. The inlet temperature of the pump also increases from 90 to 110°C and it can increase the overall efficiency by 2.73%. A considerable increment is observed of energy by 4000kW to 6800kW when the DNI increases from 600W/m^2 to 1000W/m^2. The energy destruction is also observed during the process followed at the Turbine, heat recovery steam generators (HRSG), and in the components of vapour absorption refrigeration. The exergy destruction is also identified at the central receiver of about 33%, and the next 25% in heliostat. The annual CO_2 mitigated is estimated by 1437.16MMT/year for the year 2022 in India by the application of CSP plants.

Conclusion: The result reveals tar the central receiver and heliostat of the solar field endanger the higher thermodynamics irreversibility of about 33% and 25% respectively. The trigeneration process can be utilized the low temperature for other applications, that is why the overall cycle efficiency will be increased. The trigeneration cycle with HRSG is the future technology and due to this cycle, CO_2 can also being reduced.

Keywords: solar tower, steam turbine cycle, organic, energy analysis, exergy analysis, error analysis

Citation: Parvez M, Lal S, Khan O Howari H, Siddiqui SA. An Assessment of Solar Driven Combined Cooling, Heating, and Electric Power Generation System: Using Energy, Exergy, and CO_2 Mitigation Approach. *J Mod Green Energy*, 2023; 2: 5. DOI: 10.53964/jmge.2023005.

1 INTRODUCTION

In 2023, India's installed capacity for electricity generation, which accounts for both the central and state sectors, was 412,212MW[1] as compared to the installation capacity 210,951.72MW in 2012[2]. According to the energy resources shown in the figure, the rational generation of electricity is as follows: 51.3% coal, 6.1% gas, 1.6% nuclear, 11.40% hydro, 10.20% wind, 15.6% solar, and 3.8% others. The energy sale sector-wise is 21.25% Agriculture, 31.76% Domestic, 30.74% Industrial, and 16.75 others (Public lighting, traction, public water works and sewage etc.) services, and only a little amount for transportation like electric vehicle charging.

The main source of power generation is the fossil fuel but it is not good for environment. As we now Delhi is the most populated and polluted city and it is the capital of India. To control the pollution of all the coal based power plant were permanently shut-down in national capital territory-Delhi[3] and other coal based thermal power plants in the range of 300kM to the Delhi national capital range will be closed as early as possible in the future[4]. It means the future power plants in the highly dense or populated area will be the renewable energy option in which mainly solar thermal of Photovoltaic (PV) power plant. The solar PV technology is fully matured and accepted by the peoples and government and the targeted power generation is regularly produced. But the concentrated solar power (CSP) solar thermal technology are working in India at few places now at commercial basis these are 2.5MW ACME Solar Tower (Bikaner), 14MW ISCC Plant (Dadri), 125MW Dhursar (Rajasthan), 50MW Godawari Solar Project (Nokha, Rajasthan), 100MW KVK Energy Solar Project (Askandra in Rajasthan), 50MW Megha Solar Plant (Anantapur, Andhrapradesh), 1MW National Solar Thermal Power Facility (Gurugram)[5]. This technology is most feasible and no need to sale the whole coal based thermal power plant because the much heat can be produced by the solar trough collectors, heliostat or solar towers by which steam can be produced. So many researchers are working on this technology and its integrated approaches with other like organic rankine cycle, refrigeration cycle and waste heat can be used for other industrial/domestic purposes.

Over the years, the population has been seen to be increasing drastically, which subsequently has a severe effect on the environment. The above statement can be explained as fossil fuels are being consumed at a rapid rate which creates pollution-based problems[6,7].

In addition to that the power failure in the country due to an overloaded electricity grid, the current power supply crisis, the rise the in oil and natural gas prices, and fears about energy security are all contributed to a growing interest in distributed electricity generation and on-site power generation with heat recovery[8,9]. For the last few years, there is a high degree of interest in energy

conservation means the minimization of all sorts of wastage of energy using multiple output thermodynamic systems i.e., cogeneration and trigeneration, where heat recovery and energy integration results in higher thermodynamic efficiency and reduced emissions than the separate energy systems[10].

Parvez[11] and Xie et al.[12] studied and investigated the trigeneration systems with major concern with the twin menace of rapid consumption of existing gasoline atmosphere-based degradation. To overcome these limitations, a solar-driven trigeneration system is introduced by using concentrated solar collectors which are expected to fulfil the overall energy consumption of society effectively and sustainably[13-14].

Kumar et al.[15] studied the exergy analysis of few types of solar thermal collectors and Wu et al.[16] experimentally analysed and simulated the micro combined cooling, heat and power (CCHP) system by using the thermal management controller system.

The studies on power generation technologies of conventional and non-conventional both types are mainly focused on three important parameters like energy, economic, and environmental issues[17-20]. Musharavati et al.[21] and Chaiyat and Kiatsiriroat[22] studied the CCHP integrated with organic Rankine cycle, refrigeration cycle Kalina and thermoelectric generator for enhancement of overall cycle efficiency of the system and optimized by including the three parameters that the energy, economy and environment using multi criteria optimization technique. Parvez et al.[23] thermodynamically assessed the performance of a combined power and absorption refrigeration cycle measured the exergy destruction at various points in cycle. The similar study was carried out by the Saoud et al.[24] for solar trigeneration cycle using advanced chillier.

Kerme et al.[25] studied the comprehensive thermodynamic modeling of the solar-driven LiBr-H_2O absorption chiller system. The present study examined the influenced parameters like different types of solar on the collector efficiency and useful heat gained by a collector in order to obtain the best performance. The results from the study indicated that about 71.9% of the input exergy was destructed which accounted for 84% of the total exergy loss in the collector.

Wang et al.[26] studied and compared the conventional biomass gasification of combined cooling, heating, and power system with or without the aid of solar energy. The computed results show that the CCHP system achieved average energy and exergy efficiencies of about 56% and 28%, respectively, whereas, the energy ratio of solar to biomass was approximately 0.19 in the full-load operating conditions. Parikhani et al.[27] proposed a CCHP system that was operated by an low-temperature heat source in which they used a novel ammonia-water mixture, and the proposed system is a modified version of a Kalina cycle. The computed results indicate that energy efficiency, exergy efficiency, and overall unit product cost are 49.83%, 27.68%, and 198.3 $/GJ, respectively.

More recently, Ahmad et al.[28] studied and compared the cogeneration and trigeneration energy systems. The computed results indicate that the energy output, increased from 58% to 63% when shifting the mode of operation from cogeneration to trigeneration. Further, the combined setup for the trigeneration has a higher efficiency of about 66.63% in comparison to the cogeneration cycle of about 34.5%.

In the present study, a thermodynamic analysis through energy and exergy is employed, and a comprehensive parametric study is performed to investigate the effects of various operating parameters on the performance of multiple output systems like direct normal irradiance (DNI), turbine inlet pressure, total output on an energy-based efficiency, and exergy efficiency of solar driven trigeneration system for simultaneous production CCHP.

2 MATERIALS AND METHODS

2.1 Basic Trigeneration System

Figure 1 shows a basic trigeneration energy system. This trigeneration system is an integration of an absorption-based refrigeration system in order to recover the waste heat obtained from the exit of user heat and the refrigerant employed in this system is lithium bromide combined with water or ammonia combined with water and may be taken some other absorption refrigerant mixture solutions.

2.2 Description of System Used

The basic system was designed by coupling a solar-based heliostat and centralized solar receiver with a conventional Rankine-based cycle. The conventional Rankine cycle comprises a basic heat recovery generator, a steam turbine, a condenser, and eventually a pump. Figure 2 depicts a schematic diagram of the above integration of components. The solar components comprise a heliostat base field and a centralized collector.

The molten salt absorbs all the available radiation rays which are directed toward the receiver, thereby increasing the temperature of the molten salt. This net increase in the overall temperature of molten salt is often considered a net solar gain. The superheated steam generated in the heat recovery steam generators

https://doi.org/10.53964/jmge.2023005

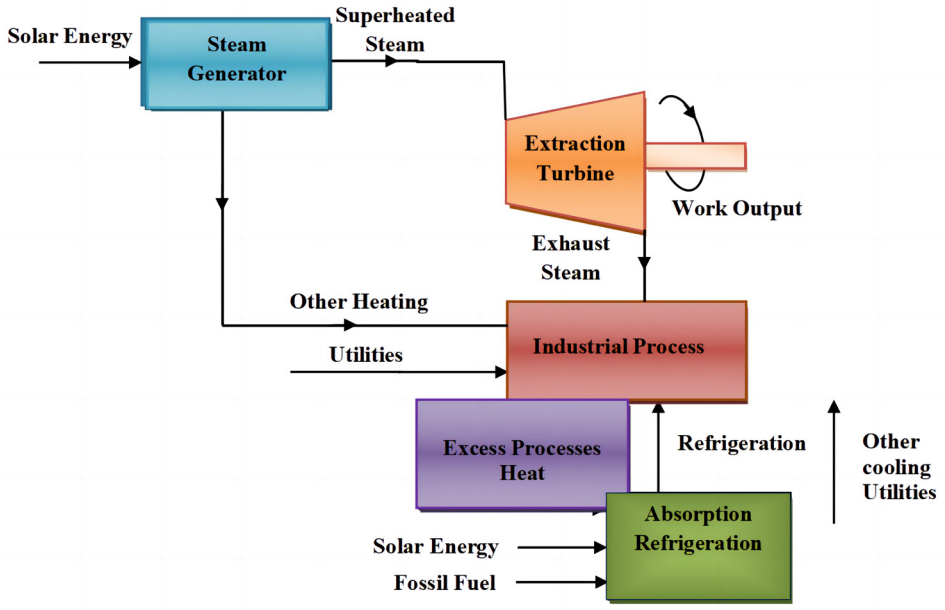

Figure 1. Schematic diagram of a solar-driven trigeneration system.

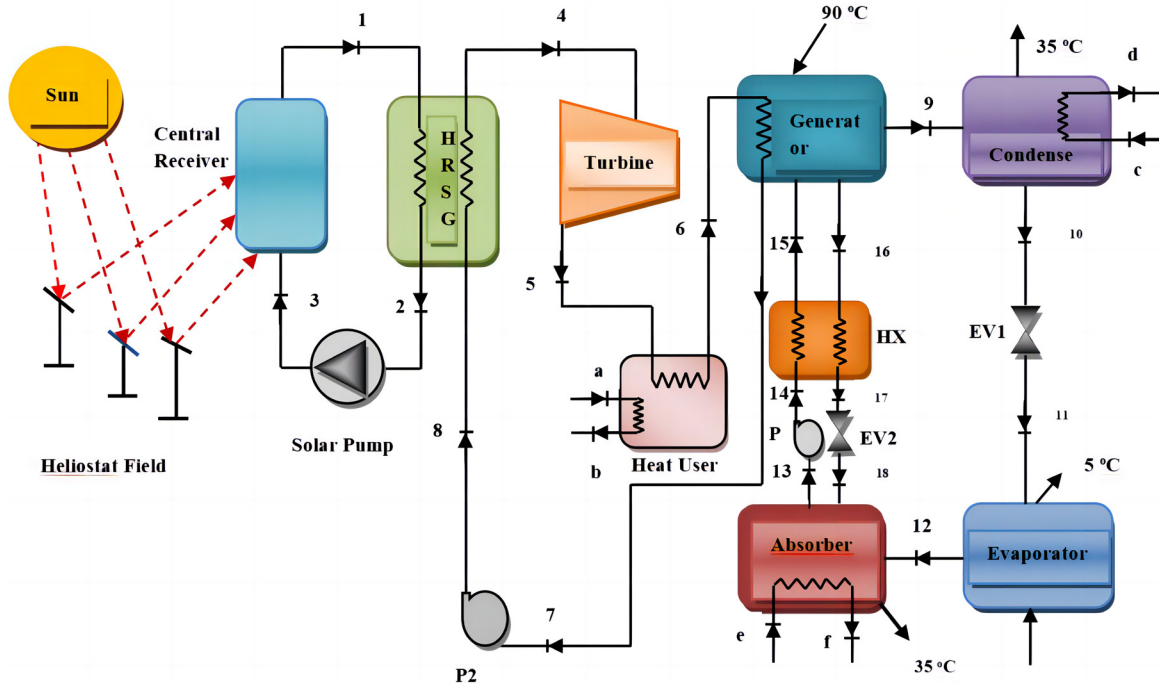

Figure 2. Solar-driven trigeneration system. EV: Electric vehicle.

(HRSG) passes through a turbine where it is expanded and produced power. The reheated steam after the partial expansion is blended and the intermediate stage for producing the process heat in the heater.

The steam at the turbine exit enters the heat user. The utilization of heat user is to reduce the temperature of the steam up to saturation stage which directs to the generator where it cooled and convert to the water that can feed to the HRSG via a feed pump.

The generator is usually employed to separate the refrigerant often water from the mixture of LiBr/H_2O with the help of steam heat. The temperature approximately 90°C attained by the solution from heat gain decides the circulation ratio of the system. As the separated refrigerant attains its required temperature, it then proceeds to the condenser of the system positioned at 9 thereby it then moves into the evaporator positioned at 11 which is subsequently boiled in it. The refrigerant leaves the evaporator at a saturated-based point at 12. This saturated state refrigerant proceeds into the absorber, where it amalgamates with the previous weak solution at point 18. Due to the above operation,

superheated heat is generated thereby enhancing the overall mixing efficiency of the system. The strong solution is then pumped at high pressure positioned at 14 which is a result of the previous mixing that happened in the system. This solution is further heated at desired temperature by utilizing a counter pass heat exchanger resulting in a subsequent weak solution positioned at 16. Further, the cooled weak solution is expanded which eventually leads to low pressure based weak solution by the application of a throttling device often with a throttling value positioned at 18.

2.3 Thermodynamic Modelling Analysis

A thermodynamic model was developed which is presented the analysis of various thermodynamic parameters of the integrated system comprising a solar-driven absorption refrigeration cycle. It is also formulated based on a cascaded system that grabs the energy and exergy methods whereas the mass, energy, and exergy would be balanced. For the majority of components to select and reduce the various irreversibilities presented in the system. The solution of the equations have been carried out by using Engineering Equation Solver software which can be computed the thermodynamic properties also. The mathematical methodology is taken from Ahmad et al.[28] and Khaliq et al[29].

To proceed the further analysis, some assumptions were made the overall process is assumed under a steady state with constant solar insulation.

- The reference environmental temperature T and pressure P are referred to be approximated 293K and 101.325KPa.
- Pressure drop and heat losses to the ambient atmosphere in a majority of components were not utilized and hence removed from the analysis.
- Subsequently, any changes registered in Kinetic based energy and potential energy are considered in the analysis.
- Any chemical reaction or chemical exergy within the system is not considered.
- The heat transfer, due to which some power is lost, is not considered in the analysis.

2.3.1 Energy Efficiency of Heliostat

The basic heliostat-associated field comprises an exceptional number of heliostats being employed to direct and concentrate the irradiation emitted from the sun to the primary receiver. Hence the total solar energy input ($\dot{Q}_{solar}$) to the system is specified as:

$$\dot{Q}_{solar} = \dot{A}_{field} q \quad (1)$$

$\dot{A}_{field}$, Area of heliostat (m^2),
q, Amount of solar radiation per unit area (W/m^2),
$\dot{Q}_{solar}$, Heat energy of solar (kW).

Where q is estimated to be the total solar irradiance emitted per meter square area and is called DNI whereas is known as the total area of the heliostat.

The primary content of thermal energy is attracted by the mirror placed in the heliostat, and further transfers this energy to the central receiver whereas the remaining energy is lost to the atmosphere and is expressed as:

$$\dot{Q}_{solar} = \dot{Q}_{CR} + \dot{Q}_{lost,\,heliostat} \quad (2)$$

$\dot{Q}_{solar}$, Heat energy of solar (kW),
$\dot{Q}_{CR}$, Heat energy of the central receiver (kW),
$\dot{Q}_{lost,\,heliostat}$, Loss of heat energy from heliostat (kW).

Thereby the overall efficiency displayed by the heliostat can be calculated as below:

$$\eta_{energy,\,heliostat} = \frac{\dot{Q}_{CR}}{\dot{Q}_{solar}} \quad (3)$$

$\eta_{energy,\,heliostat}$, Energy efficiency of heliostat (%),
$\dot{Q}_{solar}$, Heat energy of solar (kW),
$\dot{Q}_{CR}$, Heat energy of the central receiver (kW).

2.3.2 Energy Efficiency of a Central Receiver

Another content of thermal energy incoming on the central receiver is completely absorbed by the working fluid molten salt and the remaining is furnished into the atmosphere, which may be given by:

$$\dot{Q}_{CR} = \dot{Q}_{salt} + \dot{Q}_{lost,\,CR} = \dot{m}_{salt}(h_{16} - h_{15}) + \dot{Q}_{lost,\,CR} \quad (4)$$

$\dot{Q}_{CR}$, Heat energy of the central receiver (kW),
$\dot{Q}_{salt}$, Heat energy of molten salt (kW),
$\dot{m}_{salt}$, Mass flow rate of molten salt (kg/s).
$\dot{Q}_{lost,\,CR}$, Loss of heat energy from the central receiver (kW),
h, Enthalpy (kJ/kg).

The energy efficiency of a central receiver can be evaluated by:

$$\eta_{energy,\,CR} = \frac{\dot{Q}_{moltensalt}}{\dot{Q}_{CR}} \quad (5)$$

η_{energy}, Energy efficiency of a trigeneration system (%),
$\dot{Q}_{salt}$, Heat energy of molten salt (kW),
$\dot{Q}_{CR}$, Heat energy of the central receiver (kW).

2.3.3 Energy Analysis of the Trigeneration Cycle

$$\dot{Q}_P = (h_5 - h_6) \quad (6)$$

$$\dot{Q}_g = (h_6 - h_7) \quad (7)$$

$$\dot{W}_T = \dot{m}_{ST}(h_4 - h_5) \quad (8)$$

$$\dot{W}_{el} = \eta_{gen}\dot{W}_T \quad (9)$$

https://doi.org/10.53964/jmge.2023005

Table 1. Energy and Exergy Balance Equations of Each Component for the Solar-driven Trigeneration System

Component	Energy Balance Equations
HRSG	$\dot{m}_{molt.salt}(h_1 - h_2) = \dot{m}_{ST}(h_4 - h_8)$
Steam Turbine	$\dot{W}_T = \dot{m}_{ST}(h_4 - h_5)$
Heat User	$\dot{m}_{ST}(h_5 - h_6) = \dot{m}_{hw}(h_b - h_a)$
Generator	$\dot{m}_{ST}h_6 + \dot{m}_s h_{15} = \dot{m}_r h_9 + (\dot{m}_s - \dot{m}_r)h_{16} + \dot{m}_{ST}h_7$
Condenser	$\dot{Q}_c = \dot{m}_r(h_9 - h_{10}) = \dot{m}_{cw} \times c_p(T_d - T_c)$
Expansion Valve 1	$\dot{m}_{10}h_{10} = \dot{m}_{11}h_{11}$
Evaporator	$\dot{Q}_e = \dot{m}_r(h_{12} - h_{11})$
Absorber	$\dot{Q}_A = \dot{m}_r h_{12} + (\dot{m}_s - \dot{m}_r)h_{18} - \dot{m}_s h_{13}$
Pump 1	$\dot{W}_P + \dot{m}_{13}h_{13} = \dot{m}_{14}h_{14}$
Expansion Valve 2	$\dot{m}_{17}h_{17} = \dot{m}_{18}h_{18}$
Heat Exchanger	$\dot{Q}_{HX} = (\dot{m}_s - \dot{m}_r)(h_{16} - h_{17}) = \dot{m}_s(h_{15} - h_{14})$
Pump 2	$\dot{W}_P + \dot{m}_7 h_7 = \dot{m}_8 h_8$
	Exergy balance equations
HRSG	$\dot{E}_{D,HRSG} = T_0[\dot{m}_{salt}(s_2 - s_1) + \dot{m}_{st}(s_4 - s_8)]$
Steam Turbine	$\dot{E}_{D,T} = T_0\, \dot{m}_{st}(s_5 - s_4)$
Heat User	$\dot{E}_{D,H} = T_0[\dot{m}_{st}(s_6 - s_5) + \dot{m}_{cw}(s_b - s_9)]$
Generator	$\dot{E}_{D,G} = T_0[\dot{m}_r s_9 + (\dot{m}_s - \dot{m}_r)s_{16} - \dot{m}_s s_{15} - \dot{m}_{ST}(s_6 - s_7)]$
Condenser	$\dot{E}_{D,c} = \dot{m}_r[(h_9 - h_{10}) - T_0(s_9 - s_{10})] + \dot{m}_{cw}$
Expansion valve 1	$\dot{E}_{D,EV1} = T_0\dot{m}_r(s_{11} - s_{10})$
Evaporator	$\dot{E}_{D,E} = \dot{m}_r[(h_{11} - h_{12}) - T_0(s_{11} - s_{12})]$
Absorber	$\dot{Q}_A = \dot{m}_{cw}C_P(T_f - T_e)$
Pump1	$\dot{E}_{D,P1} = T_0\dot{m}_s(s_{14} - s_{13})$
Expansion Valve 2	$\dot{E}_{D,EV2} = T_0(\dot{m}_s - \dot{m}_r)(s_{18} - s_{17})$
Heat Exchanger	$\dot{E}_{D,\,HX} = T_0[\dot{m}_s(s_{15} - s_{14}) - (\dot{m}_s - \dot{m}_r)(s_{16} - s_{17})]$
Pump 2	$\dot{E}_{D,P2} = T_0\dot{m}_{st}(s_8 - s_7)$

ṁr, Mass flow rate of refrigerant (kg/s); s, Specific entropy (kJ/kg K); T_0, Ambient temperature (°C).

P, Pump,
h, Enthalpy (kJ/kg),
$\dot{Q}_P$, Process heat (kW),
η_{gen}, Electrical generator efficiency (%),
$\dot{W}_{el}$, Electrical power (kW),
$\dot{W}_T$, Turbine work (kW),
$\dot{Q}_E$, Energy of the evaporator (kW).

The overall energy efficiency of the cycle can be evaluated by:

$$\eta_{enegy} = \frac{\dot{Q}_P + \dot{Q}_e + \dot{W}_{el}}{\dot{Q}_{IN}} \quad (10)$$

η_{energy}, Energy efficiency of a trigeneration system (%),
$\dot{Q}_P$, Process heat (kW),
$\dot{W}_{el}$, Electrical power (kW),
$\dot{Q}_{IN}$, Solar energy rate input (kW).

2.3.4 Exergy Analysis of the Trigeneration Cycle

$$\dot{Q}_e = \text{C.O.P} * \dot{Q}_g \quad (11)$$

$$\dot{E}_P = \dot{m}_{hw}\ [(h_b - h_a)\ (s_b - s_a)] \quad (12)$$

$$\dot{E}_e = \dot{Q}_e\ [1] \quad (13)$$

P, Pump,
h, Enthalpy (kJ/kg),
$\dot{m}_{hw}$, Mass flow rate of hot water(kg/s).

The overall exergy efficiency of the cycle of the system can be evaluated by:

$$\eta_{exergy} = \frac{\dot{E}_P + \dot{E}_e + \dot{W}_{el}}{\dot{E}_{x,in}} \quad (14)$$

η_{exergy}, Exergy efficiency of a trigeneration system (%),
$\dot{E}_{x,\,in}$, Exergy input to the plant (kW),
$\dot{W}_{el}$, Electrical power (kW),
P, Pump.

All the formulae are shown in Table 1 which are more clarify the heat transfer, energy, and exergy mathematical relations.

Table 2. Measurement Accuracies and Experimental Uncertainties Associated with Sensors and Parameters

S. No	Sensors and Parameters	Accuracies and Uncertainties Measurement
1	Solar Radiation	±0.185W/m^2
2	T-type thermocouples	±0.21°C
3	Flow meter	±0.17mL
4	Pressure transducer	±0.14m bar
5	Voltage measurement	±0.14V
6	Current measurement	±0.14A

Table 3. Thermophysical Properties of Molten Salt[32]

Properties	Value
Density (kg/m^3)	1804
Dynamic viscosity (MPa s)	1.69
Thermal conductivity (W/m K)	0.134
Specific heat (kJ/kg K)	1.52
Upper-temperature limit (°C)	600
Lower temperature limit (°C)	220

2.4 Uncertainty Analysis

Human errors, sensor or machine faults, and measurements are taken into consideration as the main reason for uncertainties in an analysis. The perfect measurement does not exist. Despite our best efforts to reduce them, there are always going to be errors and uncertainties in every measurement. Errors and uncertainties may occur when measuring the climate, using calibration techniques, observational methods, testing solar power trigeneration systems integrated with heliostat field systems, steam turbine cycles, heat user, and vapour absorption refrigeration (VAR), and measuring global solar radiation at regular intervals.

The total uncertainties evaluating equations in the generalized form have been taken into account in the calculation for individual variables[30,31] given below:

Let us consider a general case in which an experimental result r, is a function of j measured variables X_i; than

$$r = r(X_1, X_2 \ldots\ldots\ldots\ldots, X_j) \quad (15)$$

Above Equation (15) is the data reduction equation used to determine r from the measured values of the variables X_i. Then the uncertainty in the result is given by[21]:

$$U_r = \left[\left(\frac{\partial r}{\partial X_1}\right)^2 . U_{x1}^2 + \left(\frac{\partial r}{\partial X_2}\right)^2 . U_{x2}^2 + \ldots\ldots\ldots\ldots\ldots\left(\frac{\partial r}{\partial X_j}\right)^2 . U_{xj}^2\right]^{1/2} \quad (16)$$

Where are the uncertainties in the measured variable X_i. The calculation of experimental uncertainties is carried out which is shown in Table 2.

3 RESULTS AND DISCUSSION

The study is primarily performed to understand the potential effects of various parameters like; DNI, turbine inlet pressure, total output, energy efficiency, and exergy efficiency of a solar-driven trigeneration system. The properties of molten salt have been taken from Pacio et al.[32] as shown in Table 3.

The pressure, temperature, mass flow rates, specific enthalpy, and specific entropy at various state points are presented in Table 4.

3.1 DNI in India

The Direct solar irradiance of India is shown in Figure 3 in kWh/m^2. The long term average DNI of India from 1999 to 2018 is varying between 1000 to 2350kWh/m^2 annual and it is also observed that the highest DNI found in Rajasthan and Lowest in eastern states of India[33].

This value is comes under the range of 400 to 1000W/m^2. Thats why we are taking the range of DNI between 600 to 1000W/m^2 for the various calculation in this paper. The highest DNI more than 2000 is not suitable for PV system and it can be utilised for high heat generation for which CSP technology will be adopted. The CSP technology-based power plants are situated at various places in India of generating capacity approximately 779.5MW and it will be increasing in future.

3.1.1 DNI Measurement at Faridabad, India

One day solar radiations have been measured to

https://doi.org/10.53964/jmge.2023005

Table 4. Temperature and Pressure at Various State Points for Solar-driven Trigeneration System

State Point	Pressure (bar)	Temperature (°C)	Mass Flow Rate (kg/sec)	Specific Enthalpy (kJ/kg)	Specific Entropy (kJ/kg K)
1	225	595	12.32	1580.42	7.80
2	178	290	12.32	627.80	6.98
3	178	290	12.32	627.80	9.98
4	50	500	1.7912	2433.7	6.977
5	3.172	135.5	1.7912	2727.18	6.977
6	3.172	135.5	1.7912	569.53	1.691
7	3.172	100	1.7912	419	1.307
8	3.172	101	1.7912	422	1.327
9	0.04823	90	0.1675	2660	7.480
10	0.04832	35	0.1675	175.8	0.599
11	0.00991	5	0.1675	175.8	0.6324
12	0.00991	5	0.1675	2510.7	9.0270
13	0.00991	35	2.011	187.98	0.23827
14	0.04832	35	2.011	187.98	0.23827
15	0.04832	70.5	2.011	168.15	0.42789
16	0.04832	90	1.8434	211.56	0.4912
17	0.04832	53.4	1.8434	150.27	0.30811
18	0.00991	53.4	1.8434	150.27	0.30811

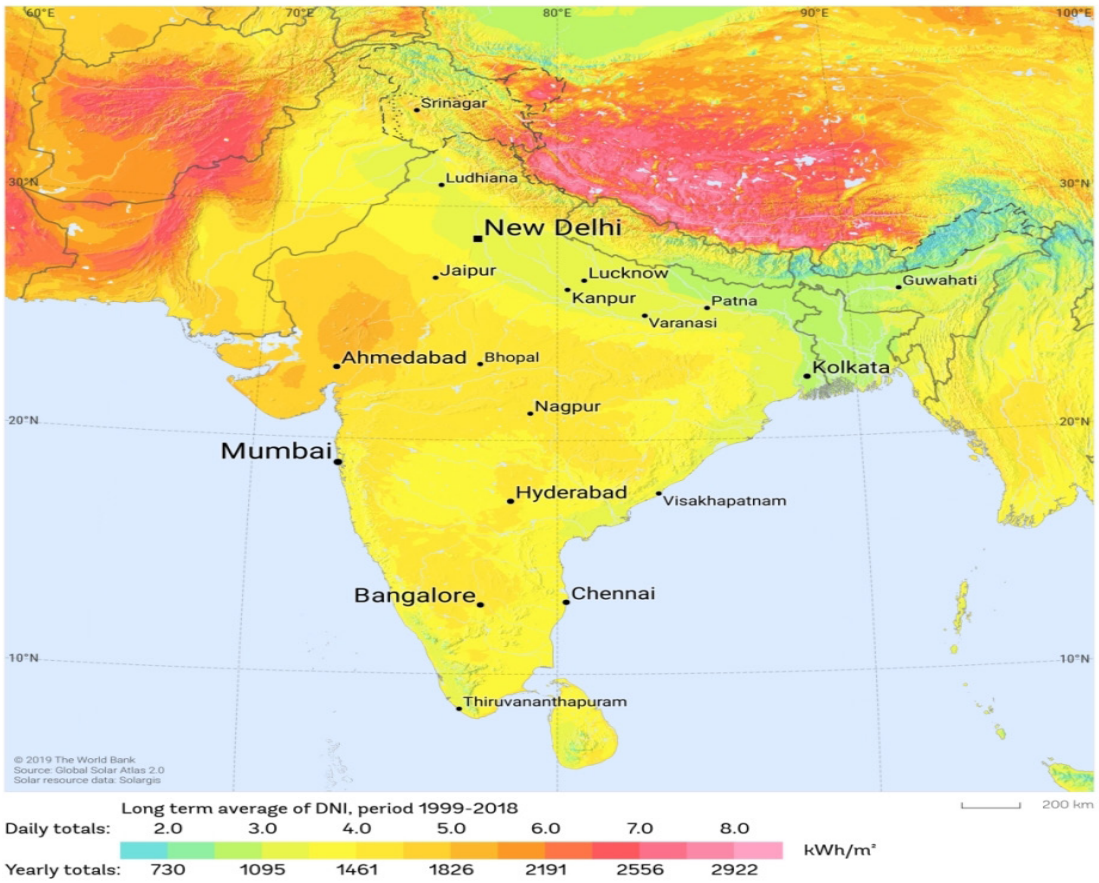

Figure 3. Map of DNI of India[33].

verify the solar DNI availability in Faridabad on March 04, 2023 as shown in Figure 4. The average DNI is approximately 601W/m^2. The highest DNI is observed at 12 noon by 885W/m^2 and the lowest DNI is observed at evening 6PM by 12W/m^2. A CMP3model of Kippzonen make Pyranometer was used to measure

https://doi.org/10.53964/jmge.2023005

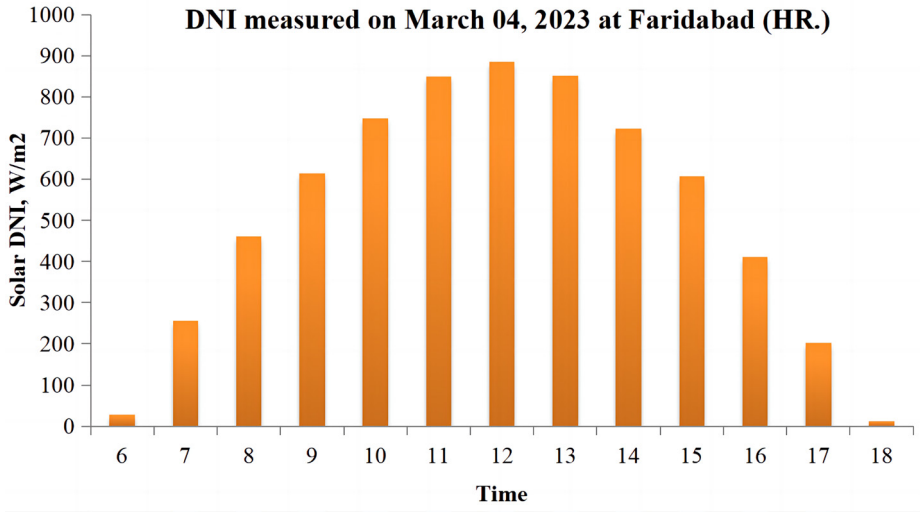

Figure 4. DNI on March 04, 2023 at Faridabad, India.

the solar irradiance. The measuring range for DNI of the equipment is upto 2000W/m^2. The sensitivity of the instrument is 10-32μv/W/m^2. The operating temperature range is -20℃ to +80℃. The K-type thermocouple was used to measure the weather temperature. An eight channel data logger was used to store the data. The range of the DNI is comes under the range used in the analysis of the solar driven combined cooling, heating, and electric power generation system.

3.2 Energy and Exergy Analysis of Trigeneration Efficiency VS Change in DNI

Figure 5 illustrated the variation in energy and exergy efficiency when the DNI changed from (600-1000W/m^2). It is observed the notable increase in cogeneration efficiency for all DNI varies in the range of 32 to 35%. The VAR was employed to produce cooling with power and process heat affects the efficiency and the total efficiency is raised to 65%.

This significant enhancement in efficiency was observed due to a large amount of cooling production presented at the evaporator. Since both process heat and cooling capacity are the quantity of energy production at the evaporator and heater. Further, the simultaneous production of electric power rate of process heat and rate of cooling production at the expense of solar radiation falling on the heliostat provides very high conversion efficiency, and hence the system is called trigeneration and has been found quite efficient from the energy point of view.

3.3 Energy and Exergy Analysis of Trigeneration Efficiency VS. Change in Pump Inlet Temp

Figure 6 shows the exergetic performance of the system for subsequent variations in pump inlet temperature. The figure clarifies that the increase in the temperature of the system will improve energy-based efficiency. Further any subsequent rise in the temperature at the inlet of a pump (90℃-110℃) endangers the energy efficiency by a small percentage but enhances the exergy efficiency of the trigeneration system by 2.73%. These enhancements in energy and exergy efficiencies of trigeneration occur primarily due to the subsequent increase in pump entry temperature reducing the amount of heat required at the generator of VAR which increases the cooling effect. It means enhances the overall performance of the system.

3.4 Variation in a Change of DNI VS. Exergy Destruction

Figure 7 shows the variation in the magnitude of exergy destruction in the key components of the trigeneration system with a change of DNI. It is observed that exergy destruction in the turbine increases significantly as the DNI increases. Moreover, the exergy destruction in the HRSG, process heater, and VAR has shown increasing trends for all the selected values of DNI. More significant variation of exergy destruction was observed in the turbine which is from 900kW to 1600kW when the DNI changes from 600W/m^2 to 1000W/m^2. This deviation describes considerable non-isentropic expansion steam in the turbine at larger values of DNI.

A considerable enhancement in the exergy destruction at HRSG is observed due to large entropy generation via heat transfer a finite temperature difference with the increased value of DNI. A similar reason was observed for the enhancement in exergy destruction at the process heater. The exergy destruction in the components of VAR is least affected by the change of DNI due to the reason its effect is diluted after going through various processes of energy conversion between the heliostat

https://doi.org/10.53964/jmge.2023005

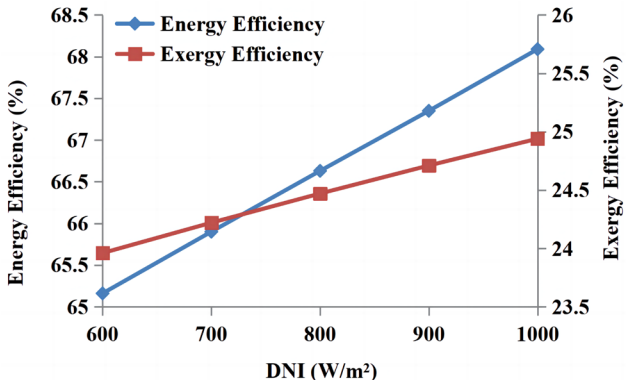

Figure 5. Variation in energy and exergy efficiency vs. change in DNI.

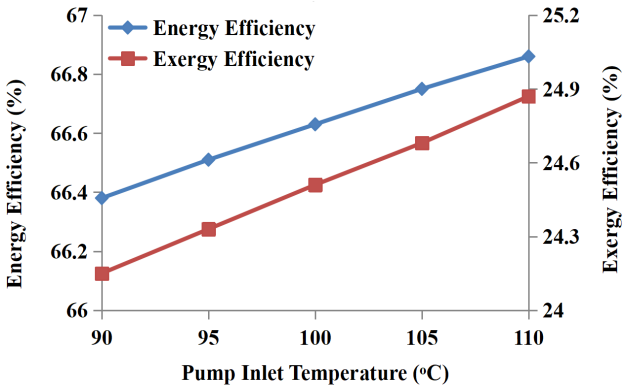

Figure 6. Variation in energy and exergy efficiency vs. change in pump inlet temperature.

field and VAR.

3.5 Total Energy and Exergy Output

The individual energy and exergy output of a trigeneration system and its variation with change in DNI was seen which is displayed in a graph in Figure 8. It has been observed that the combined energy and exergy-based output enhances considerably with a subsequent variation in DNI, it rises from (4000kW to 7000kW and 1400kW to 2400kW) when the DNI is enhanced between (600W/m^2 to 1000W/m^2). This increasing trend is due to the reason that process heat output increases very significantly as the DNI increases. Comparatively the overall heat acquired is higher than the overall heat acquired by electrical, power, and cooling. A simultaneous increase in three energy outputs of the cycle increased its overall energy and exergy output.

In view of highlighting the exergy assessment advantages over the energy traditional approach, a bar chart displaying a clear comparison of energy and exergy efficiency of the three individual cycles has been plotted in Figure 9.

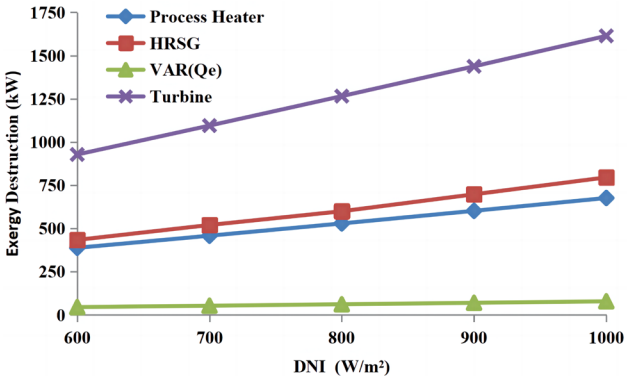

Figure 7. Variation in a change of DNI vs. exergy destruction.

3.6 Exergy Destruction in the Trigeneration Cycle

Figure 10 illustrate the percentage of exergy destruction of different components of the proposed system observed. From the computed results, the maximum exergy destruction was noted in a central receiver of about 33%, and the next 25% in heliostat. In addition, a sum of 24% was produced as an exergetic output, consisting of 15% turbine power, 7.5% accompanied by process heat, and 1.5% accompanied by cooling capacity.

3.7 CO_2 Mitigation

The power generation installed capacity from CSP for India is 779.5MW in year 2022 The data for CSP power plant is taken from the source[5].The specific coal consumption perkWh was estimated by Mittal et al.[34] to be 0.77kg/kWh, and For the purpose of calculating a specific coal consumption, we used the same value. According to studies of Kaushik et al.[35], Singh et al.[19] and Lal et al.[20] the average CO_2 equivalent for energy is 0.98 kg/kWh CO_2. The total coal required to produce 779.5MW is 1752.63MMT/year. In India to produce the equivalent power from the coal based power plant the annual CO_2 emission is estimated by 1437.16MMT/ year it means it is mitigated, the use of solar energy (a clean energy fuel) is intended to minimize. It is stated that adopting CSP for electricity generation can help to mitigate global warming by preventing the vast amount of carbon dioxide creation.

4 CONCLUSION

A theoretical framework developed through the combined application of energy and the exergy analyses of thermodynamics for the design and development of a steam turbine-based trigeneration. The proposed trigeneration system running on solar thermal energy has opened the door for engineers and scientists to harness this solar thermal potential of a given region and to promote the concept of sustainable energy technology. Results obtained after the combined application of the

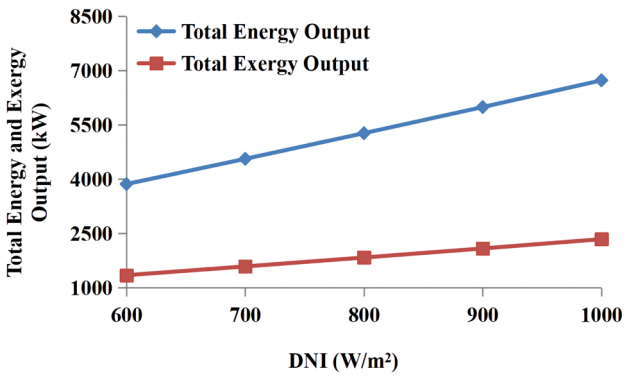

Figure 8. Variation in a change in DNI vs. total energy and exergy output.

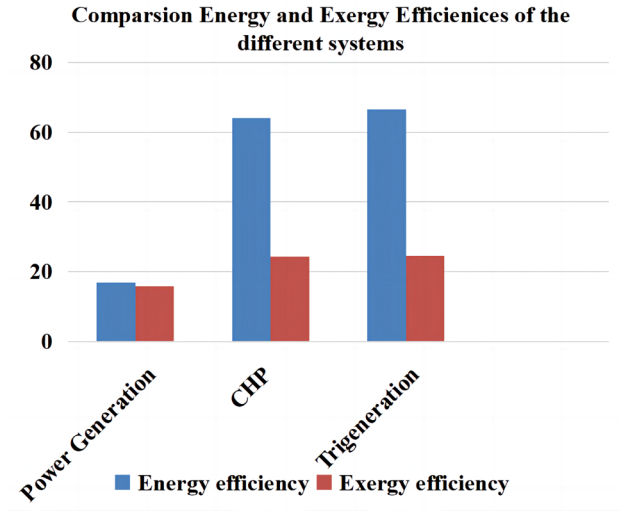

Figure 9. Comparison of energy and exergy efficiencies of different systems.

energy and exergy analyses may be summarized as:

1. A slight gain in the energy and exergy efficiencies was observed after a considerable increase in the value of DNI from (600W/m^2-1000W/m^2).

2. It is shown that a rise in pump inlet temperature from 90°C to 110°C endangers the energy efficiency by less than a percent but enhances the exergy efficiency of the trigeneration system by 2.73%.

3. It is observed that the combined energy output increases considerably with the increase of DNI, it rises from 4000kW to 6800kW when the DNI increases from 600W/m^2 to 1000W/m^2.

4. The exergy destruction out of 100% exergy of the cycle, the maximum exergy destruction was noted in a central receiver of about 33%, and the next 25% in heliostat respectively.

5. The annual CO_2 mitigated is estimated by 1437.16MMT/year for the year 2022 in India by the application of CSP plants.

Acknowledgements
Not applicable.

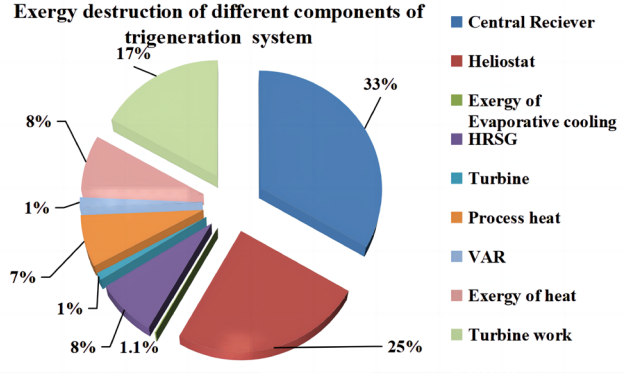

Figure 10. Exergy destruction of different components of the trigeneration system.

Conflicts of Interest

The authors declared no competing interests.

Author Contribution

Parvez M was responsible for the conceptualization; Lal S was responsible for writing, reviewing, and editing; Khan O was responsible for content writing; Howari H was responsible for diagram, software, and data; Siddiqui SA was responsible for methodology development.

Abbreviation List

CCHP, Combined cooling, heat and power
CSP, Concentrated solar power
DNI, Direct normal irradiance
HRSG, Heat recovery steam generators
PV, Photovoltaic
VAR, Vapour absorption refrigeration

References

[1] Power generation. Assessed April 02, 2023. Available at:[Web]

[2] Lal S, Kumar P, Rajora R. Performance analysis of photovoltaic based submersible water pump. IJET, 2013; 5: 552-560.

[3] India. Shut all 11 NCR thermal plants to curb pollution: Delhi to Centre. Accessed April 05, 2023. Available at:[Web]

[4] India. Temporary shut down of power plants around Delhi helped reduce pollution. Accessed April 05, 2023. Available at:[Web]

[5] India. Concentrating solar power (CSP) projects in India, Accessed April 05, 2023. Available at:[Web]

[6] Balat M. Coal-fired power generation: proven technologies and pollution control systems. Energ Source Part A, 2007; 30: 132-140.[DOI]

[7] Atilgan B, Azapagic A. Life cycle environmental impacts of electricity from fossil fuels in Turkey. J Cleaner Prod, 2015; 106: 555-564.[DOI]

[8] Jouhara H, Khordehgah N, Almahmoud S et al. Waste heat recovery technologies and applications. Therm Sci Eng Prog, 2018; 6: 268-289.[DOI]

[9] Zoghi M, Habibi H, Chitsaz A et al. Exergoeconomic analysis of a novel trigeneration system based on organic quadrilateral cycle integrated with cascade absorption-compression system for waste heat recovery. Energ Convers Manage, 2019; 198: 111818.[DOI]

[10] Khalid F, Kumar R, Khalid F. Feasibility study of a new solar based trigeneration system for fresh water, cooling, and electricity production. Int J Energ Res, 2021; 45: 19500-19508.[DOI]

[11] Parvez M. Thermodynamic analysis of a biomass gasifier driven combined power and ejector-absorption refrigeration (CPER) system. Int J Exergy, 2019; 29: 69-88.[DOI]

[12] Xie N, Xiao Z, Du W et al. Thermodynamic and exergoeconomic analysis of a proton exchange membrane fuel cell/absorption chiller CCHP system based on biomass gasification. Energy, 2023; 262: 125595.[DOI]

[13] Murugan M, Saravanan A, Elumalai PV et al. An overview on energy and exergy analysis of solar thermal collectors with passive performance enhancers. Alex Eng J, 2022; 61: 8123-8147.[DOI]

[14] Ahmad S, Parvez M, Khan TA et al. A hybrid approach using AHP-TOPSIS methods for ranking of soft computing techniques based on their attributes for prediction of solar radiation. Environ Challenges, 2022; 9: 100634.[DOI]

[15] Kumar S, Kumar A, Maithani R et al. Exergy analysis of various solar thermal collectors. Mater Today: Proc, 2022; 69: 323-327.[DOI]

[16] Wu JY, Wang JL, Li S et al. Experimental and simulative investigation of a micro-CCHP (micro combined cooling, heating and power) system with thermal management controller. Energy, 2014; 68: 444-453.[DOI]

[17] Majid MA, Kumar JCR. Renewable energy for sustainable development in India: current status, future prospects, challenges, employment, and investment opportunities. Energy Sustain Soc, 2020; 10: 1-36.[DOI]

[18] Zhang L, Xu M, Chen H et al. Globalization, green economy and environmental challenges: state of the art review for practical implications. Front Env Sci, 2022; 10: 199.[DOI]

[19] Singh A, Lal S, Kumar N et al. Role of nuclear energy in carbon mitigation to achieve United Nations net zero carbon emission: evidence from Fourier bootstrap Toda-Yamamoto. Environ Sci Pollut R, 2023; 30: 46185-46203.[DOI]

[20] Lal S, Babu Balam N, Jain HK. Performance evaluation, energy conservation potential, and parametric study of borehole heat exchanger for space cooling in building. J Renew Sustain Ener, 2014; 6: 023123.[DOI]

[21] Musharavati F, Khanmohammadi S, Pakseresht AH et al. Enhancing the performance of an integrated CCHP system including ORC, Kalina, and refrigeration cycles through employing TEG: 3E analysis and multi-criteria optimization. Geothermics, 2021; 89: 101973.[DOI]

[22] Chaiyat N, Kiatsiriroat T. Analysis of combined cooling heating and power generation from organic Rankine cycle and absorption system. Energy, 2015; 91: 363-370.[DOI]

[23] Parvez M, Khalid F, Khan O. Thermodynamic performance assessment of solar-based combined power and absorption refrigeration cycle. Int J Exergy, 2022; 31: 232-248.[DOI]

[24] Saoud A, Bruno JC, Boukhchana Y et al. Performance analysis and assessment of a highly energy-integrated solar trigeneration system using advanced absorption chillers. 2022; 474-482.

[25] Kerme ED, Chafidz A, Agboola OP et al. Energetic and exergetic analysis of solar-powered lithium bromide-water absorption cooling system. J Clean Prod, 2017; 151: 60-73.[DOI]

[26] Wang J, Ma C, Wu J. Thermodynamic analysis of a combined cooling, heating and power system based on solar thermal biomass gasification ☆ . Appl Energy, 2019; 247: 102-115.[DOI]

[27] Parikhani T, Azariyan H, Behrad R et al. Thermodynamic and thermoeconomic analysis of a novel ammonia-water mixture combined cooling, heating, and power (CCHP) cycle. Renew Energy, 2020; 145: 1158-1175.[DOI]

[28] Ahmad S, Parvez M, Khan TA et al. Performance comparison of solar-powered cogeneration and trigeneration systems via energy and exergy analyses. Int J Exergy, 2022; 39: 395-409.[DOI]

[29] Khaliq A, Alharthi MA, Alqaed S et al. Analysis and assessment of tower solar collector driven trigeneration system. J Sol Energ, 2020; 142: 051003.[DOI]

[30] Coleman HW, Steele WG. Experimentation, Validation, and Uncertainty Analysis for Engineers, Experimentation, Validation, and Uncertainty Analysis for Engineers. John Wiley & Sons, Inc.: Hoboken, NJ, USA, 2009.[DOI]

[31] Holman JP. Experimental methods for engineers, Eighth Edition. Tata McGraw Hill, Series in Mechanical Engineering: New York, USA, 2012.

[32] Pacio J, Singer C, Wetzel T et al. Thermodynamic evaluation of liquid metals as heat transfer fluids in concentrated solar power plants. Appl Therm Eng, 2013; 60: 295-302.[DOI]

[33] India. Direct Normal Irradiance. Assessed April 6, 2023. Available at:[Web]

[34] Mittal ML, Sharma C, Singh R. Estimates of emissions from coal fired thermal power plants in India: 2012 International emission inventory conference. 2012.

[35] Kaushik SC, Garg T, Lal S. Thermal performance prediction and energy conservation potential of earth air tunnel heat exchanger for thermal comfort in building. J Renew Sustain Ener, 2014; 6: 013107.[DOI]